CALET observation of gamma rays

Masaki Mori
Ritsumeikan University
For the CALET collaboration

"Synergies at New Frontiers at Gamma-rays, Neutrinos and Gravitational Waves"
ICRR, 24-25 March 2022

The CALET collaboration

O. Adriani[1,2], Y. Akaike[3,4], K. Asano[5], Y. Asaoka[5], E. Berti[1,2],G. Bigongiari[6,7], W.R. Binns[8] , M. Bongi[1,2], P. Brogi[6,7], A. Bruno[9], J.H. Buckley[8], N. Cannady[10,11.12], G. Castellini[13], C. Checchia[6,7], M.L. Cherry[14], G. Collazuol[15,16], K. Ebisawa[17], A.W. Ficklin[14], H. Fuke[17], S. Gonzi[1,2] , T.G. Guzik[14], T. Hams[10], K. Hibino[18], M. Ichimura[19], K. Ioka[20], W. Ishizaki[5], M.H. Israel[8], K. Kasahara[21], J. Kataoka[22], R. Kataoka[23], Y. Katayose[24], C. Kato[25], Y. Kawakubo[14], N. Kawanaka[20,26], K. Kobayashi[3,4], K. Kohri [27], H.S.Krawczynski[8], J.F. Krizmanic[11], P. Maestro[6,7], P.S. Marrocchesi[6,7], A.M. Messineo[7,28], J.W. Mitchell[11], S. Miyake[29], A.A. Moiseev[11,12,30], M. Mori[31], N. Mori[2], H.M. Motz[32], K. Munakata[25], S. Nakahira[17], J. Nishimura[17], G.A de Nolfo[9], S. Okuno[18], J.F. Ormes[33], N. Ospina[15,16], S. Ozawa[34], L. Pacini[1,2,13], P. Papini[2], B.F. Rauch[8], S.B. Ricciarini[2,13], K. Sakai[10,11,12], T. Sakamoto[35], M. Sasaki[11,12,30] Y. Shimizu[18], A. Shiomi[36], P. Spillantini[1], F. Stolzi[6,7], S. Sugita[35], A. Sulaj[6,7], M. Takita[5], T. Tamura[18], T. Terasawa[5], S. Torii[3], Y. Tunesada[37], Y. Uchihori[38], E.Vannuccini[2], J.P. Wefel[14], K. Yamaoka[39], S. Yanagita[40], A. Yoshida[35], K. Yoshida[21] and W.V. Zober[8] (81)

1) University of Florence, Italy
2) INFN of Florence, Italy
3) RISE, Waseda University, Japan
4) JEM Utilization Center, JAXA, Japan
5) ICRR, University of Tokyo, Japan
6) University of Siena, Italy
7) INFN of Pisa, Italy
8) Washington University-St. Louis, USA
9) Heliospheric Physics Lab., NASA/GSFC, USA
10) CSST, University of Maryland, USA
11) Astroparticle Physics Lab., NASA/GSFC, USA
12) CRESST, NASA/GSFC, USA
13) IFAC,CNR, Italy
14) Louisiana State University, USA
15) University of Padova
16) INFN of Padova, Italy
17) ISAS, JAXA , Japan
18) Kanagawa University, Japan
19) Hirosaki University, Japan
20) YITP, Kyoto University, Japan
21) Shibaura Institute of Technology, Japan
22) SASE, Waseda University, Japan
23) National Institute of Polar Research, Japan
24) Yokohama National University, Japan
25) Shinshu University, Japan
26) Dept. of Astronomy, Kyoto University, Japan
27) IPNS, KEK, Japan
28) University of Pisa, Italy
29) Ibaraki, National College of Technology, Japan
30) Dept. of Astronomy, University of Maryland, USA
31) Ritsumeikan University, Japan
32) GCSE, Waseda University, Japan
33) University of Denver, USA
34) NICT, Japan
35) Aoyama Gakuin University, Japan
36) Nihon University, Japan
37) Osaka City University, Japan
38) QST, Japan
39) Nagoya University, Japan
40) Ibaraki University, Japan

See Torii-san’s talk for overview of CALET results

CALET/CAL schematics

Fully active thick calorimeter ($30X_0$) optimized for electron spectrum measurements well into TeV region

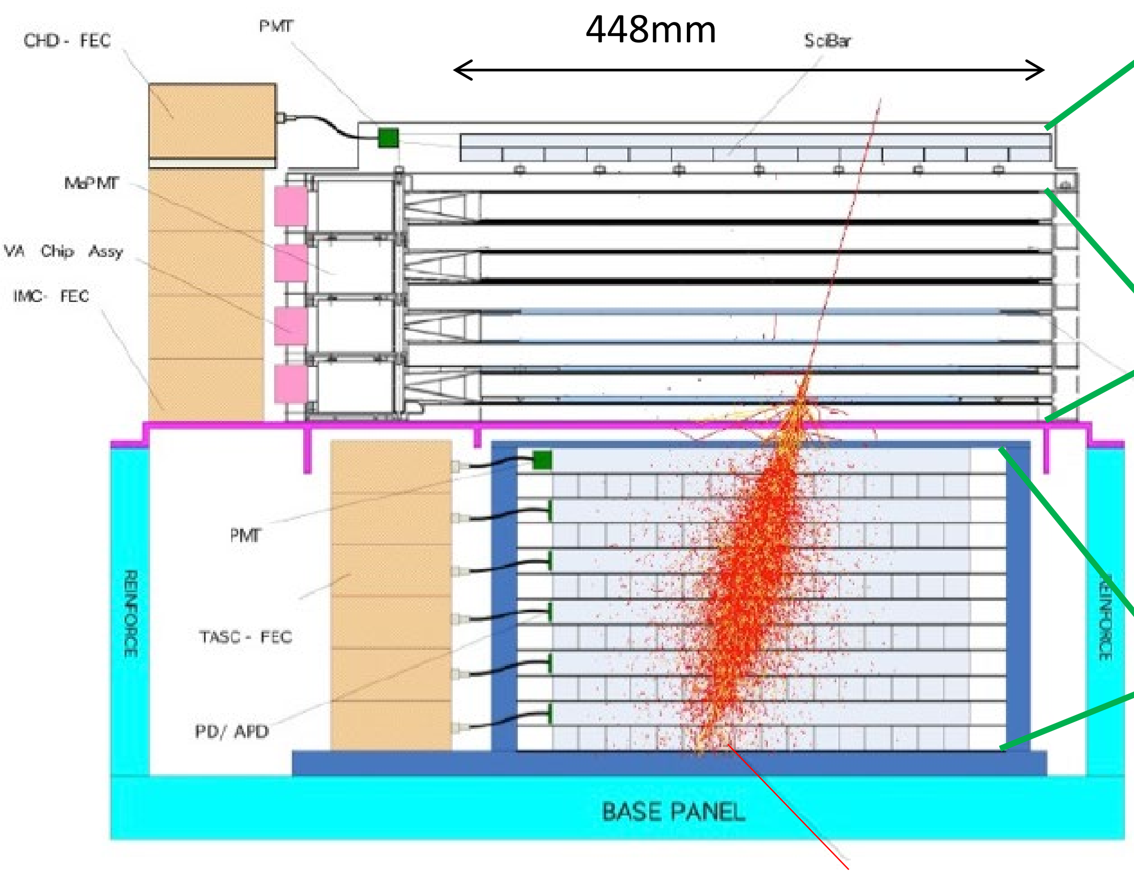

1TeV electron shower is fully contained in TASC

Charge Detector **CHD**

plastic scintillator hodoscope,
absolute charge measurement
(including charge zero)

Imaging Calorimeter **IMC**

SciFi + tungsten plate ($3X_0$),
reconstruction of arrival direction and initial shower development

Total Absorption Calorimeter **TASC**

PWO hodoscope ($27X_0$),
energy measurements and particle identification

Overview of CALET/CAL Trigger System

Y. Asaoka et al., Astroparticle Phys. 100, 29 (2018)

High Energy Shower Trigger (HE)

- High energy electrons (10GeV ～20TeV)
- High energy gamma rays (10GeV ～10TeV)
- Nuclei (a few10GeV～1000TeV)

Low Energy Shower Trigger (LE)

- Low energy electron at high latitude (1GeV ～10GeV)
- GeV gamma-rays originated from GRB (1GeV ～)
- Ultra heavy nuclei (combined with heavy mode)

Single Trigger (Single)

- For detector calibration : penetrating particles (mainly non-interacting protons and heliums)

(*) In addition to above 3 trigger modes, heavy modes are defined for each of the above trigger mode. They are omitted here for simple explanation.

Auto Trigger (Pedestal/Test Pulse)

- For calibration:
  - ADC offset measurement (Pedestal)
  - FEC's response measurement (Test pulse)

Trigger rate dependence on ISS position

Y. Asaoka et al., Astroparticle Phys. 100, 29 (2018)

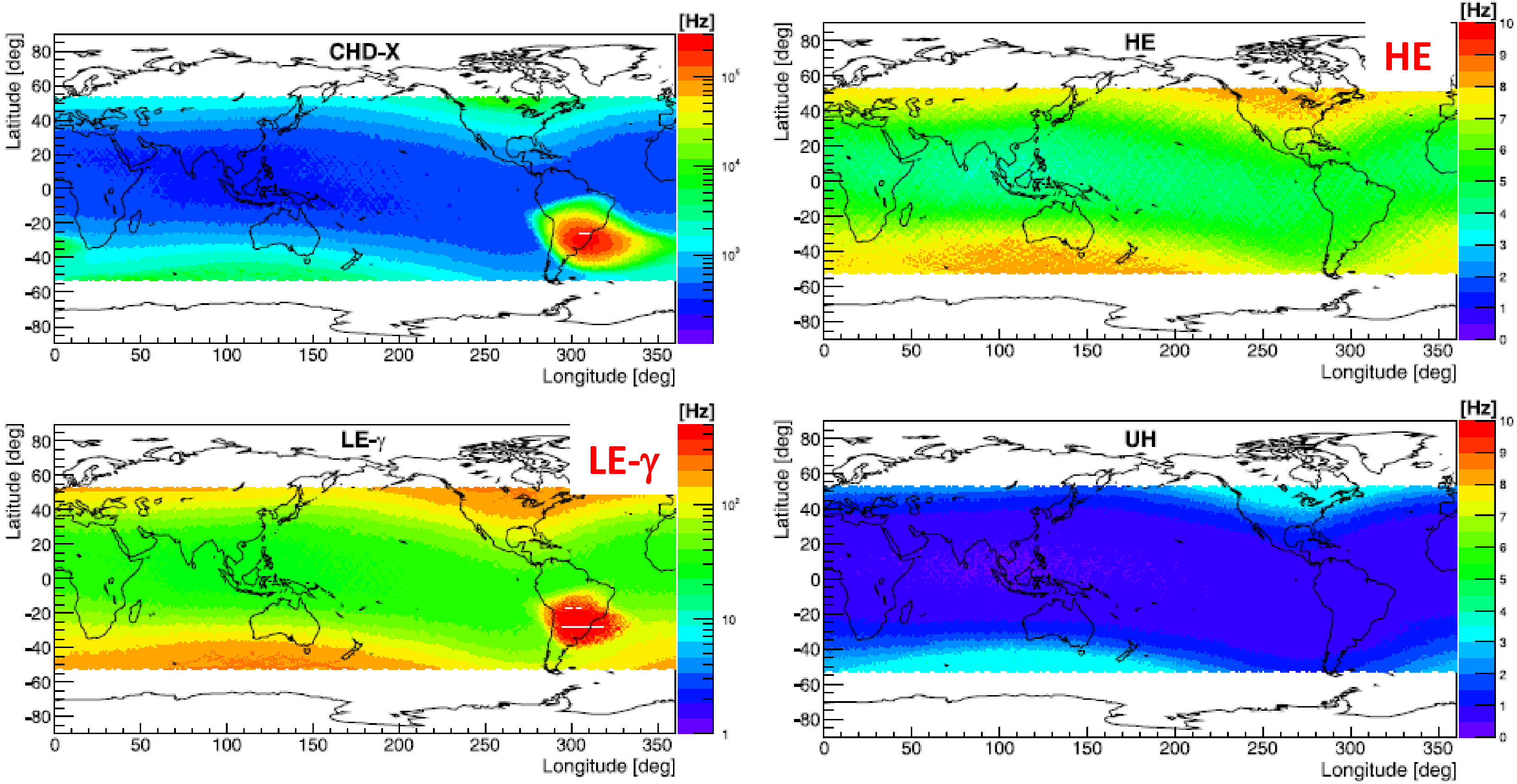

Fig. 6. Trigger/count rate dependence on the ISS position. From top to bottom, the CHD-X count rate, LE-γ trigger rate, HE trigger rate, and UH trigger rate are shown as color maps. While the LE-e trigger is selected at the highest geomagnetic latitude, the maximum trigger rate is below 100 Hz, because of the requirements of LD hits in the upper detector layers. Note that the rate range in the color map is selected for each trigger mode so that the dependence on the geomagnetic latitude is clear.

Event Examples of High-Energy Showers

Electron, E=3.05 TeV

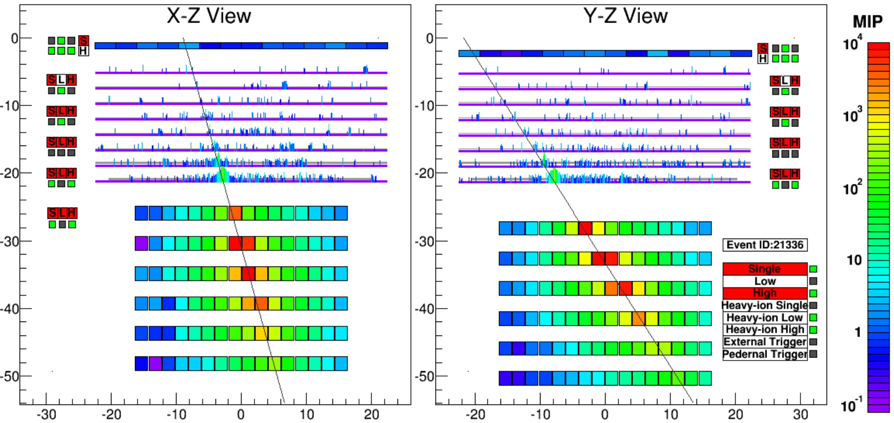

fully contained even at 3TeV

Proton, ΔE=2.89 TeV

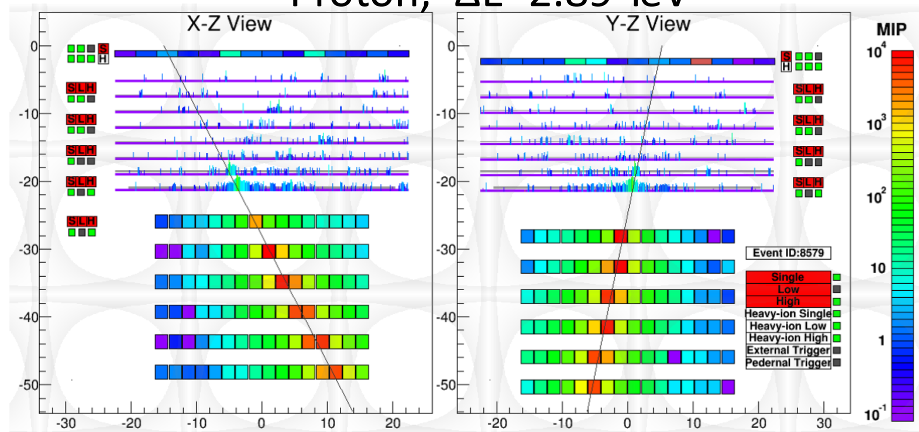

clear difference from electron shower

Fe(Z=26), ΔE=9.3 TeV

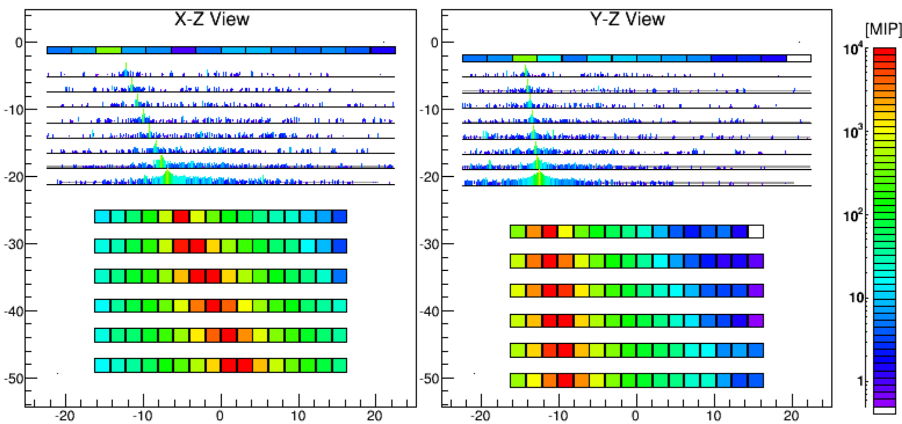

energy deposit in CHD consistent with Fe

Gamma-ray, E=44.3 GeV

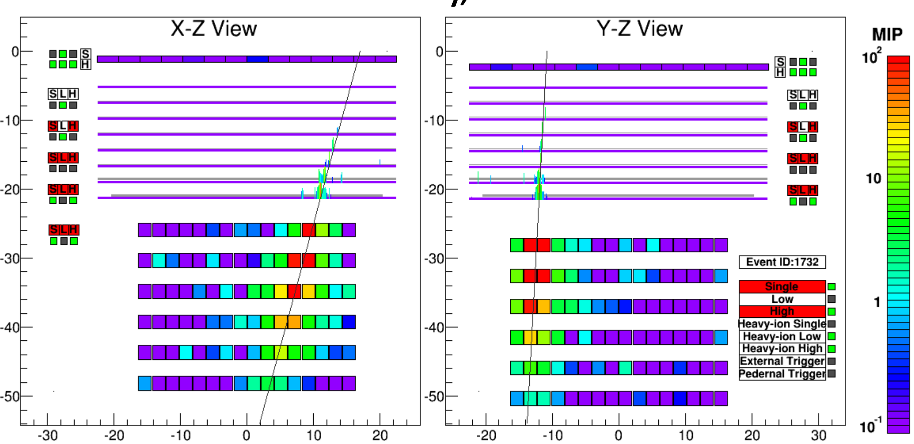

no energy deposit before pair production

Gamma Ray Event Identification

Cannady et al., ApJS 238:5 (2018)

= Electron Selection Cut + Gamma-ray ID Cut w/ Lower Energy Extension

100 GeV Event Examples

gamma-ray | electron | proton

Charge Z=0 | Charge Z=1

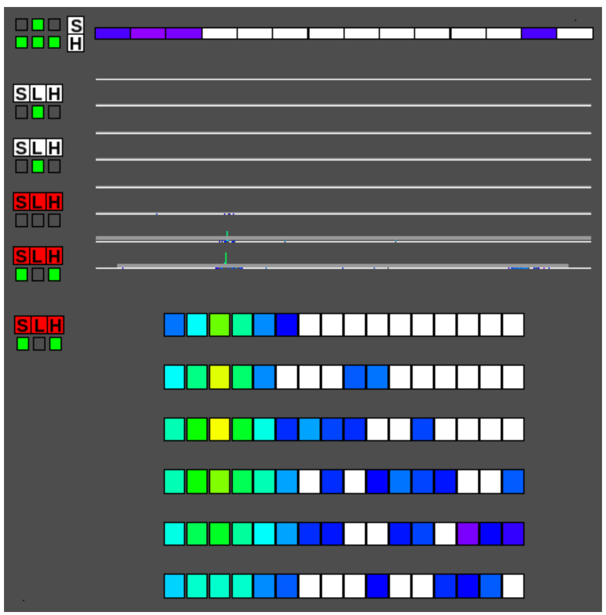

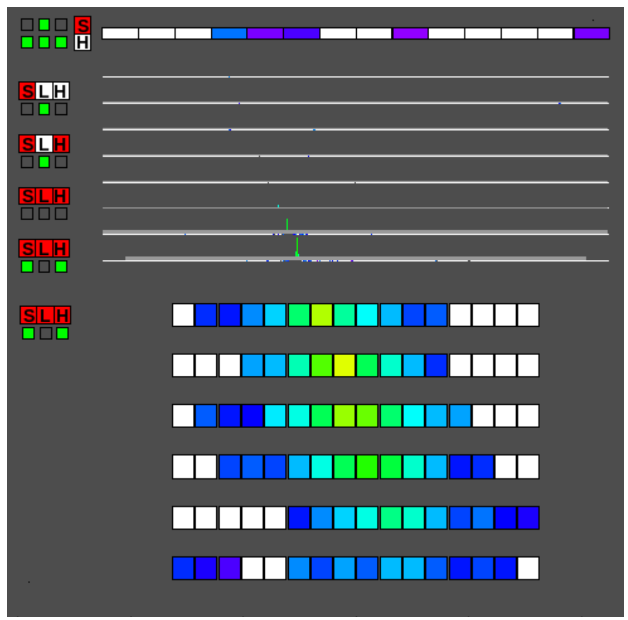

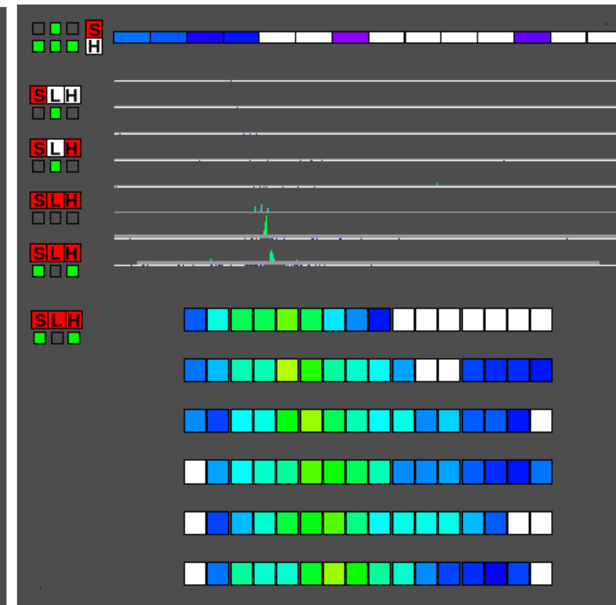

Electromagnetic Shower | Hadron Shower

well contained, constant shower development | larger spread

Gamma Ray Event Selection in CAL

= Electron Selection Cut + Gamma-ray ID Cut w/ Lower Energy Extension

It was found that secondary gamma rays produced in ISS structures are dominant source of background

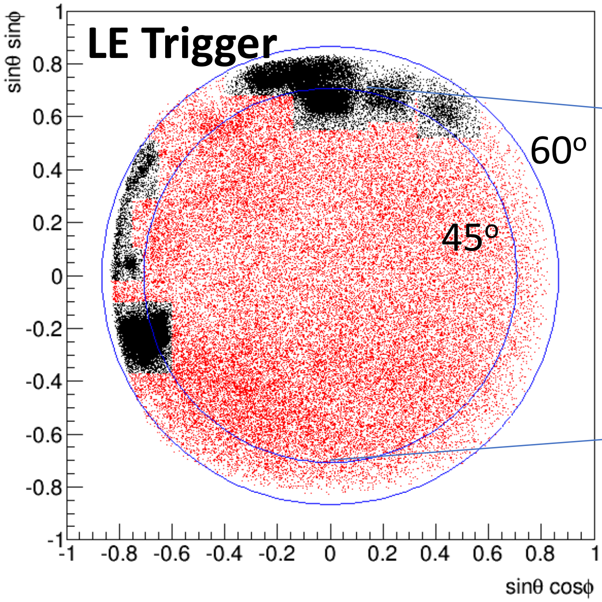

Gamma-ray candidates in CALET FOV

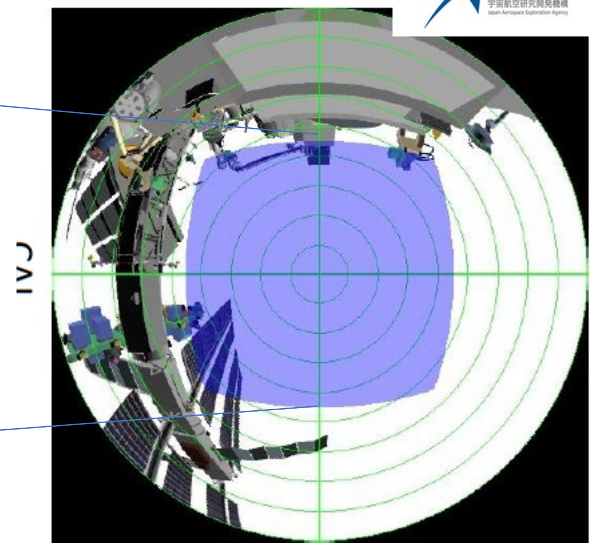

Fish-eye view of CALET FOV

By removing Black parts, it is possible to reject majority of such background. More sophisticated rejection method is under development.

1. Geometry Condition
   - CHD-Top to TASC 1st layer (2cm margin)
2. Preselection
   - Offline trigger
   - Shower concentration
   - Shower starting point
3. Track quality cut
   - Track hits >2
   - matching w/ TASC
4. Electromagnetic shower selection
   - shower shape
5. Gamma-ray ID
   - CHD-veto
6. FOV cut

Improved Gamma Ray Event Selection

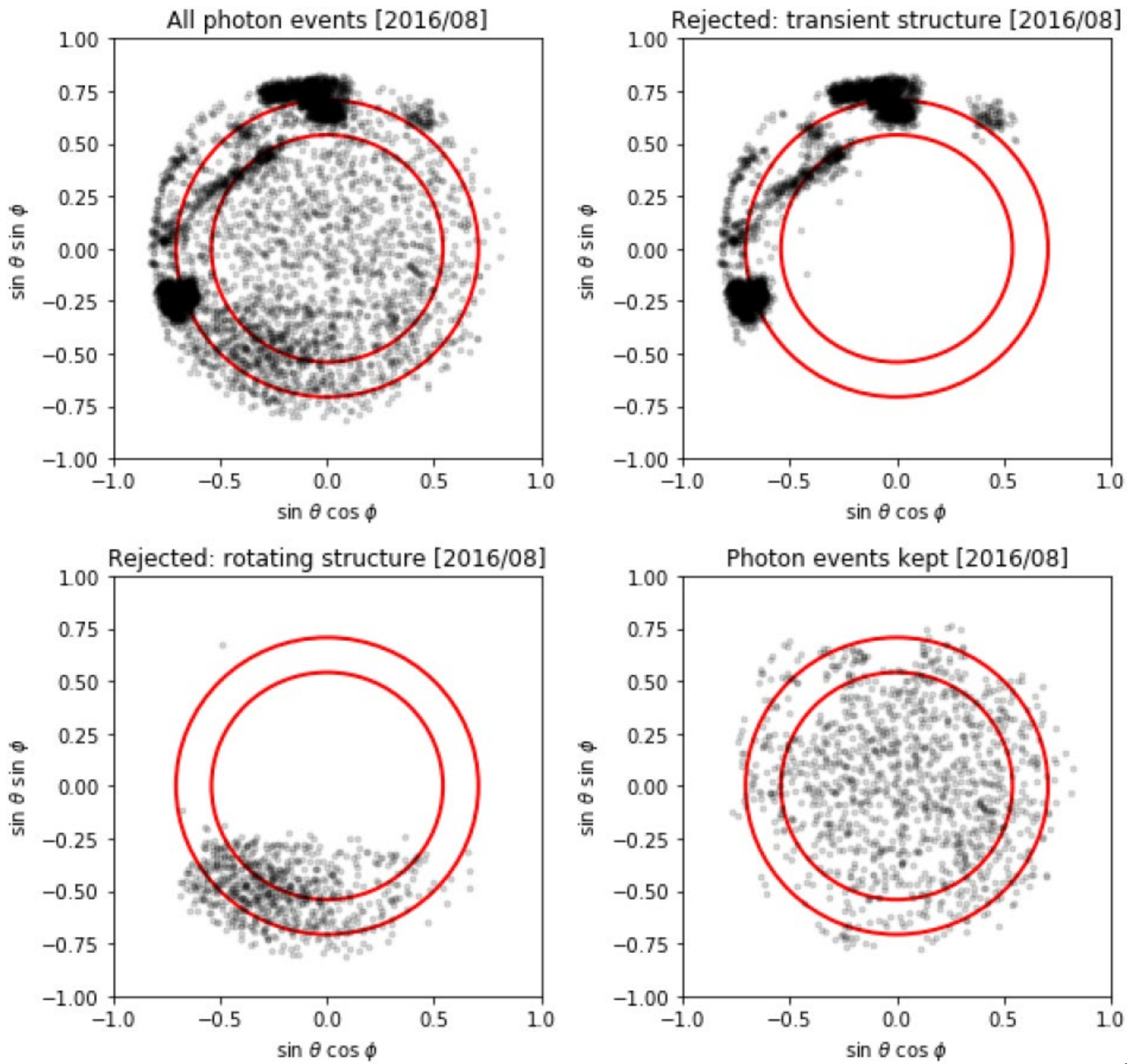

One month of gamma-ray candidates with various obstructions. Clockwise from upper left: all candidates; candidates removed by manually defined cuts; candidates removed as coming from rotating structures; events kept after FOV cuts. Red circles: 45° and 60° from zenith.

Cannady et al., PoS (ICRC2021)

Point spread function (PSF)

Cannady et al., ApJS 238:5 (2018)

$$P(\theta_s) = f_{core} K(\theta_s, \sigma_{core}, \gamma_{core}) + (1 - f_{core}) K(\theta_s, \sigma_{tail}, \gamma_{tail}) \qquad K(\theta_s, \sigma, \gamma) = \frac{1}{2\pi\sigma^2}\left(1 - \frac{1}{\gamma}\right)\left[1 + \frac{1}{2\gamma}\frac{\theta_s^2}{\sigma^2}\right]^{-\gamma}$$

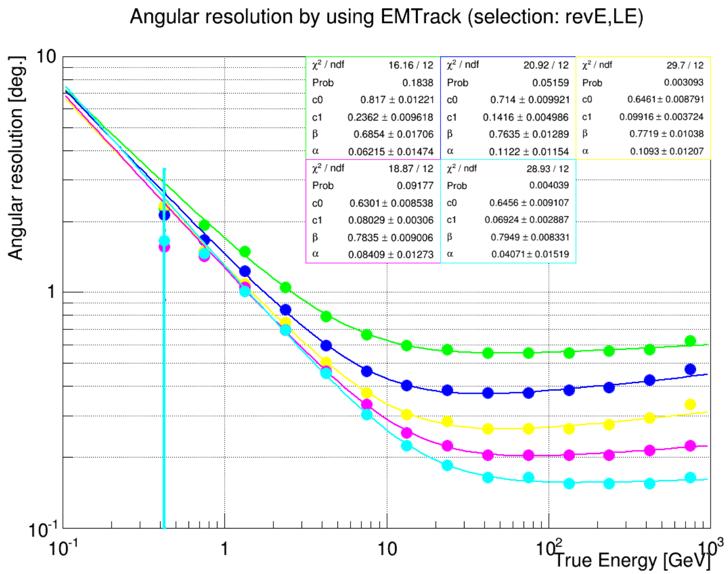

N_p : number of track points used for reconstruction

Np=3 Np=4 Np=5
Np=6 Np=7

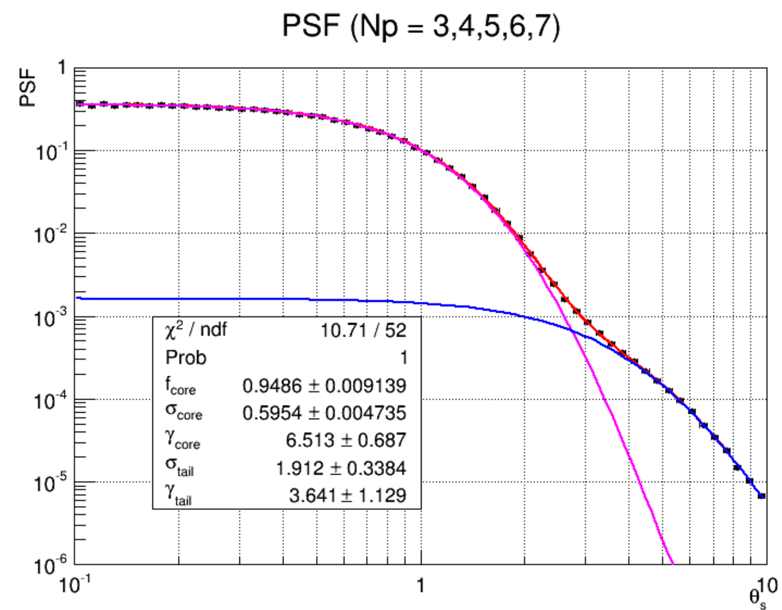

core
tail
core + tail

CALET performance

- HE trigger (>10 GeV) is always active in normal observations
- LE-γ trigger (>1 GeV) mode is activated when the geomagnetic latitude is below 20° or following a CALET Gamma-ray Burst Monitor (CGBM) burst trigger

Energy resolution

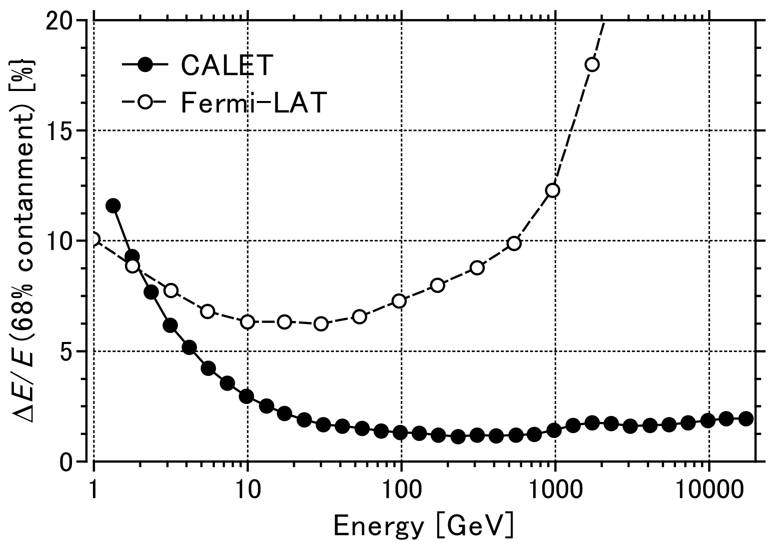

Asaoka et al, Astropart. Phys. 91, 1 (2017)

Effective area (for gamma rays)

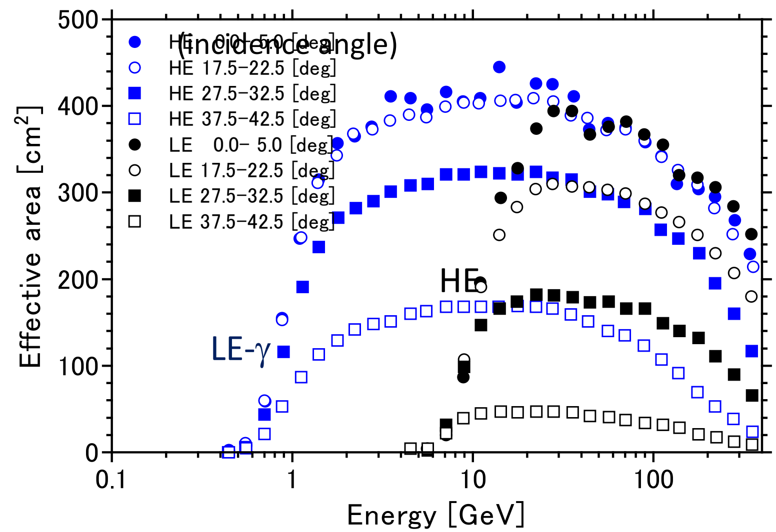

Cannady et al., ApJS 238, 5 (2018)

- Good energy resolution at high energies thanks to the thick calorimeter!

Skymap (LE-γ trigger, >1 GeV)

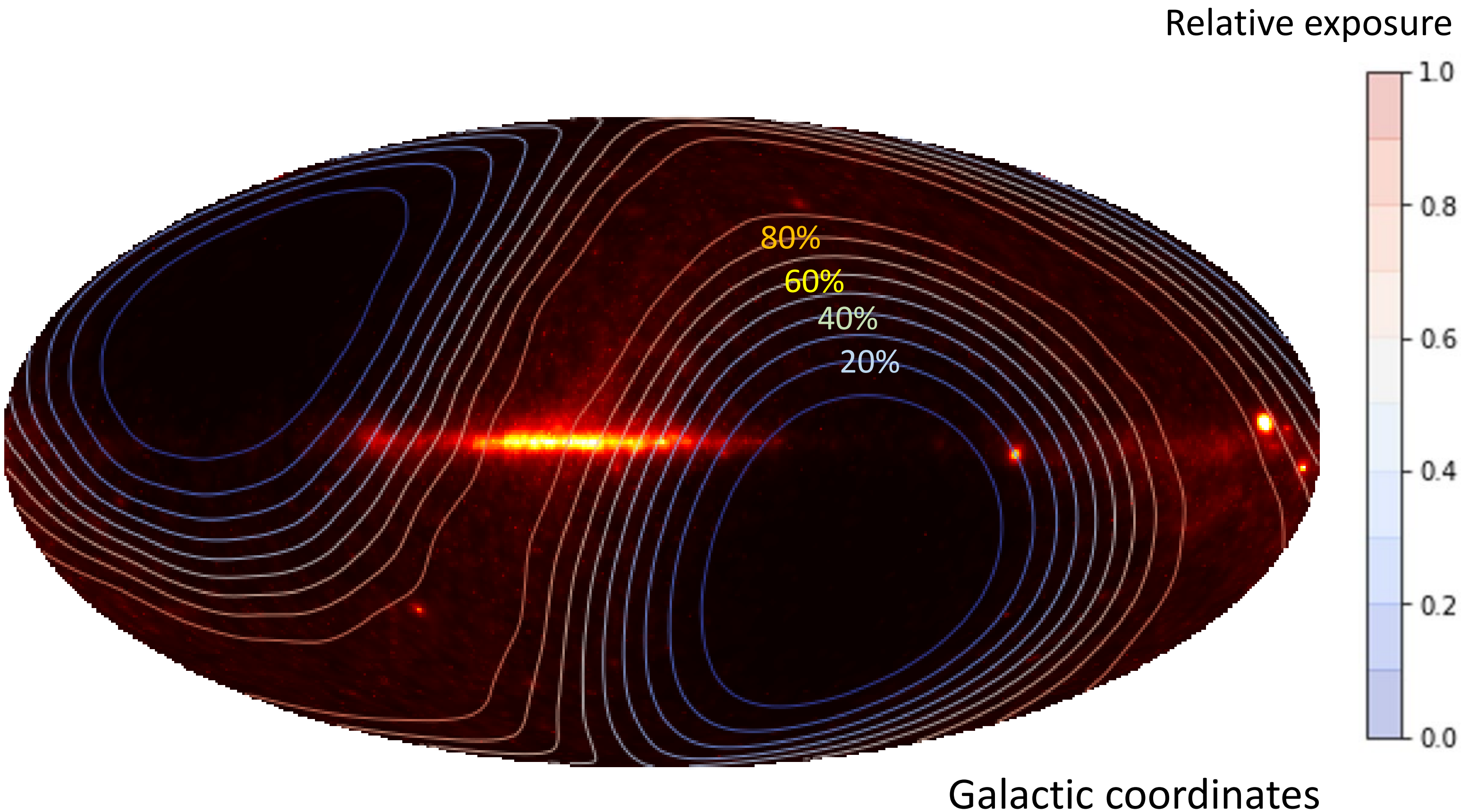

- Exposure is not uniform due to the ISS orbit (inclination 51.6°)

Point sources (LE-γ trigger, >1 GeV)

Preliminary

October 13, 2015 – September 30, 2020

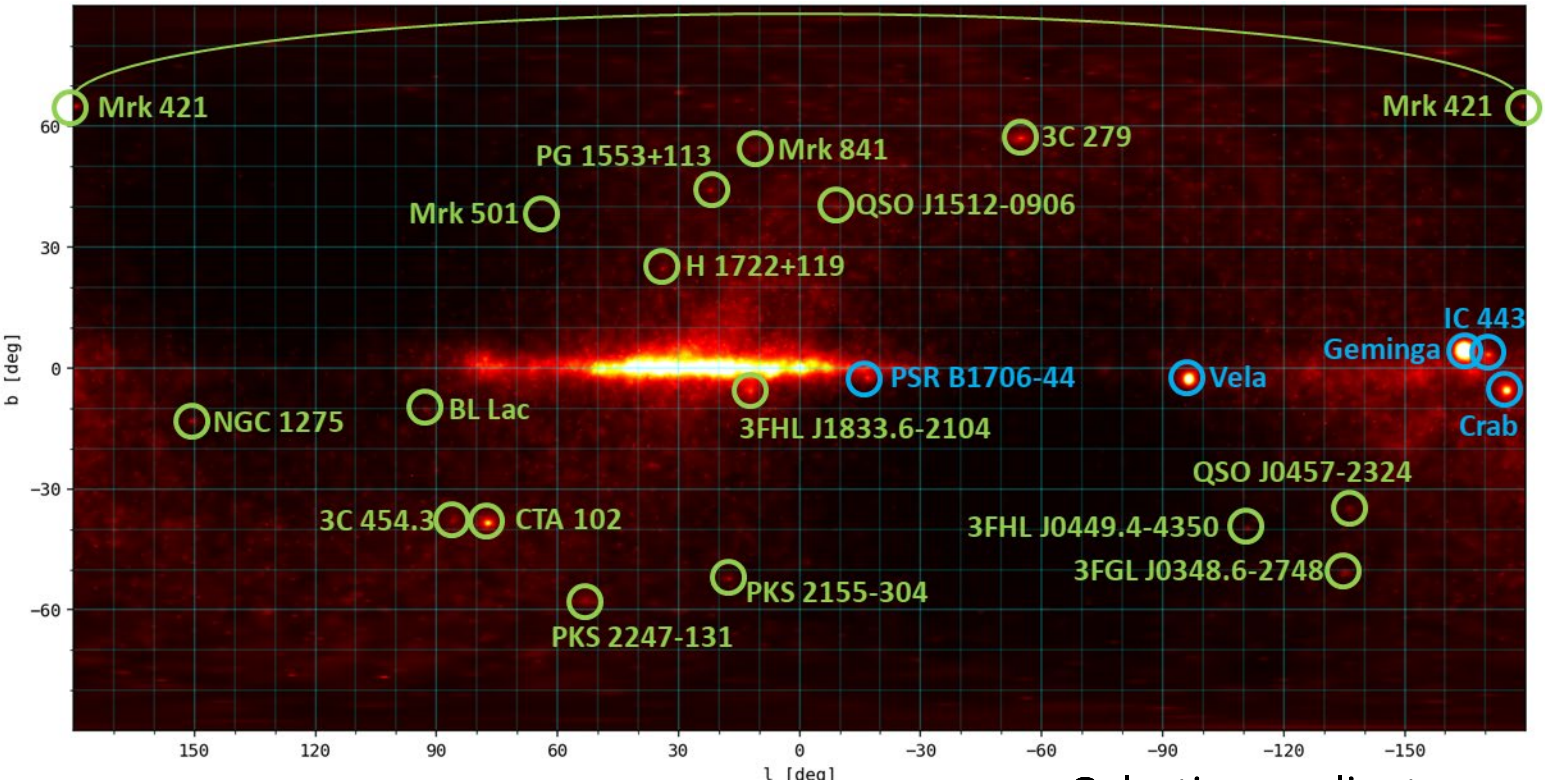

Galactic coordinates

- >20 point sources (Crab, Geminga, Vela, CTA102,…) have been detected.

See PoS (ICRC2021) 619 for LE-γ results

Skymap (HE-γ trigger, >10 GeV)

Preliminary

October 13, 2015 – September 30, 2020
110,855 gamma-ray candidates

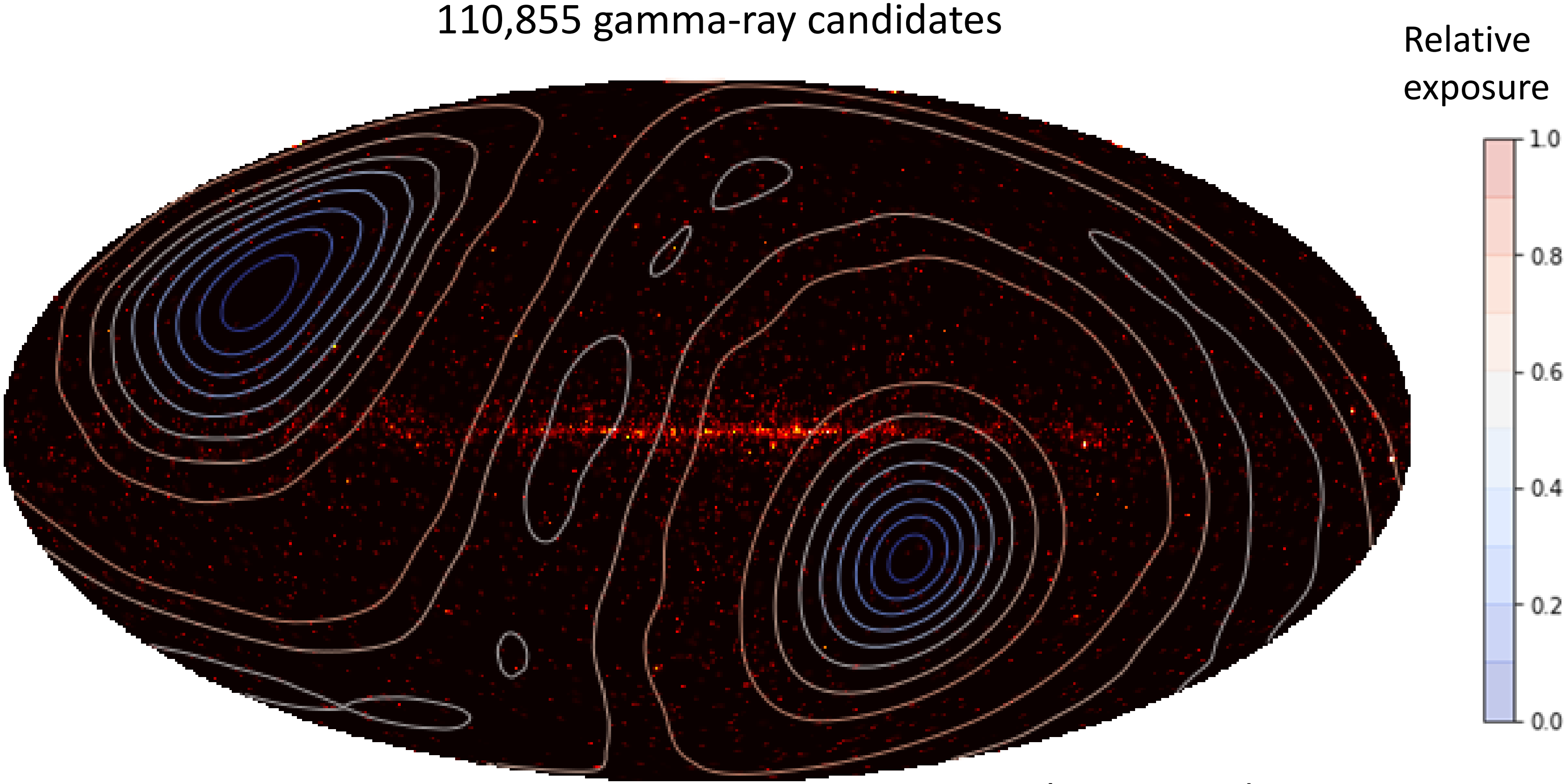

Galactic coordinates

- Exposure is not uniform due to the ISS orbit (inclination 51.6°)

Skymap (HE-γ trigger, >10 GeV)

(Fermi data: analyzed from public data.)

Preliminary

October 13, 2015 – September 30, 2020

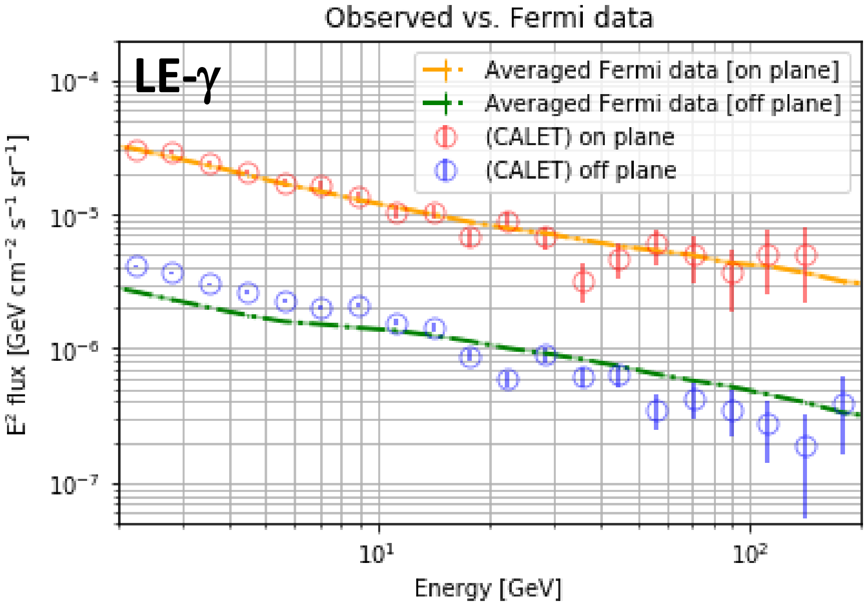

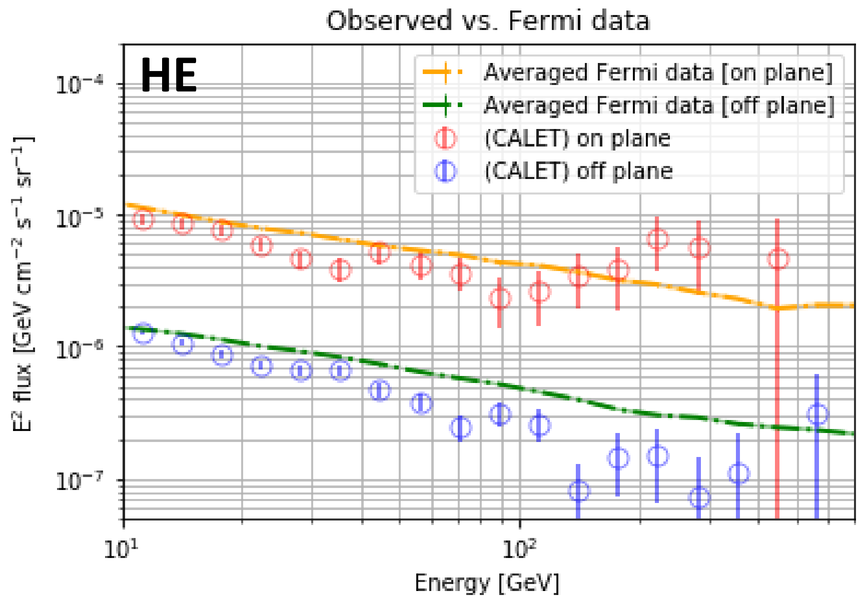

"**On-plane**": $|l| < 80°$ & $|b| < 8°$, "**Off-plane**": $|b| > 8°$

- The spectra (Galactic diffuse + point sources) look fairly consistent with those by Fermi-LAT.

Bright Galactic sources

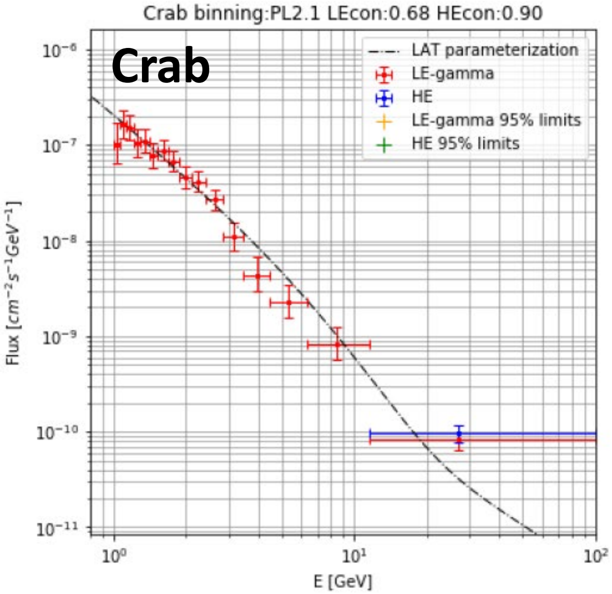

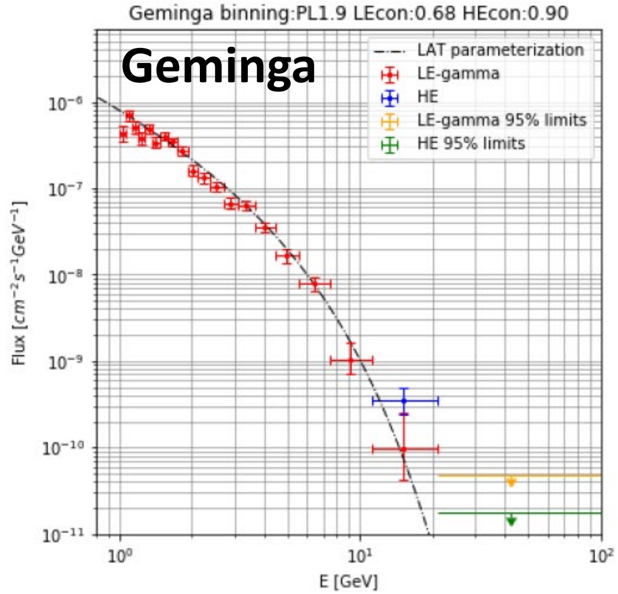

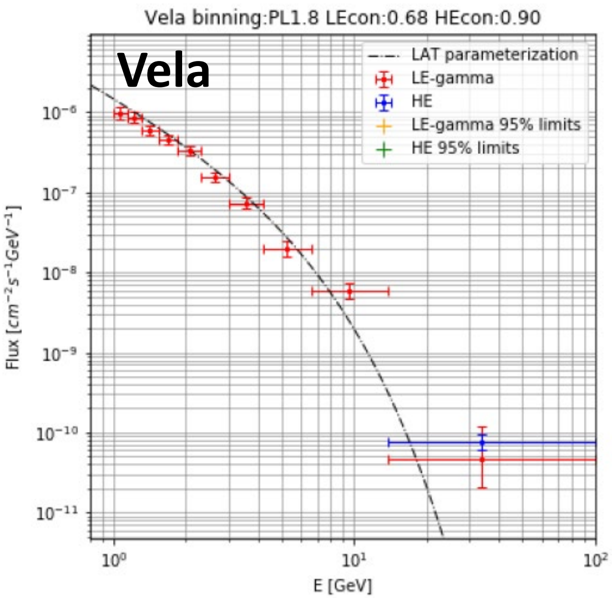

Fluxes from Crab, Geminga, and Vela based on five years of CALET observations. They are consistent within errors with fits published by Fermi LAT Collaboration shown by dashed lines.

Cannady et al., PoS (ICRC2021)

Line signals from dark matter interaction

Annihilation: $\chi\,\chi \rightarrow \gamma\,\gamma$ etc., E_γ = m_χ

T. Bringmann, C. Weniger / Dark Universe 1 (2012) 194–217

Note that generally the branching ratio into $\gamma\gamma$ suffers suppression (< 10^{-3}).

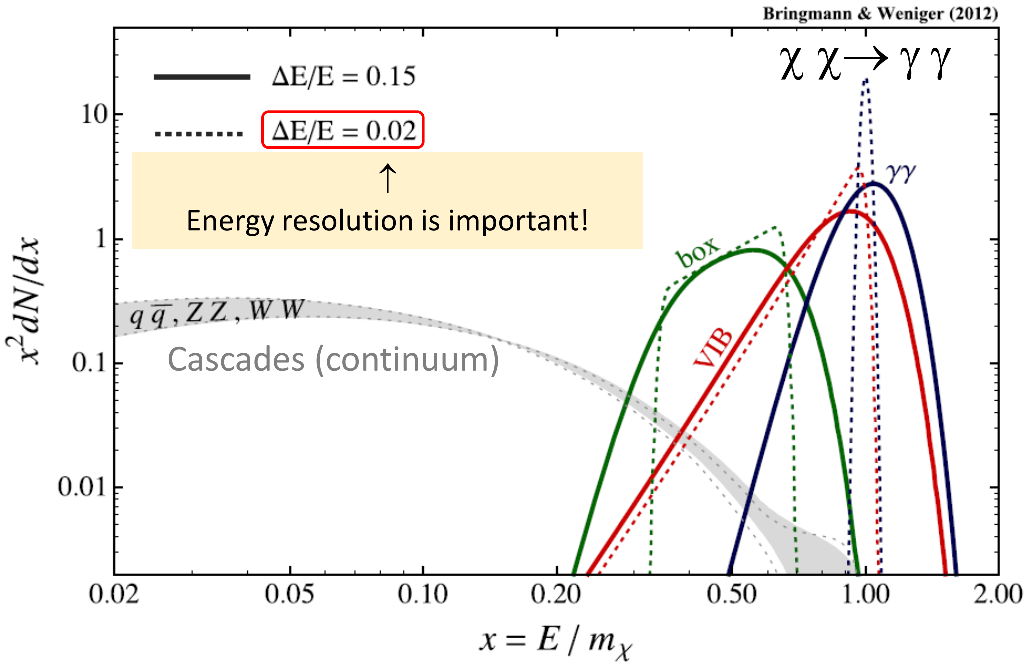

VIB (Virtual internal bremsstrahlung)

Decay: $\chi \rightarrow \gamma\,\nu$ etc., E_γ = $m_\chi/2$

Ibarra and Tran, PRL 100, 061301 (2008)

Dark matter distribution

- Dark matter halo is associated with our Galaxy and distributes spherically.
- Typical velocity: $v \sim O(10^{-3})c$

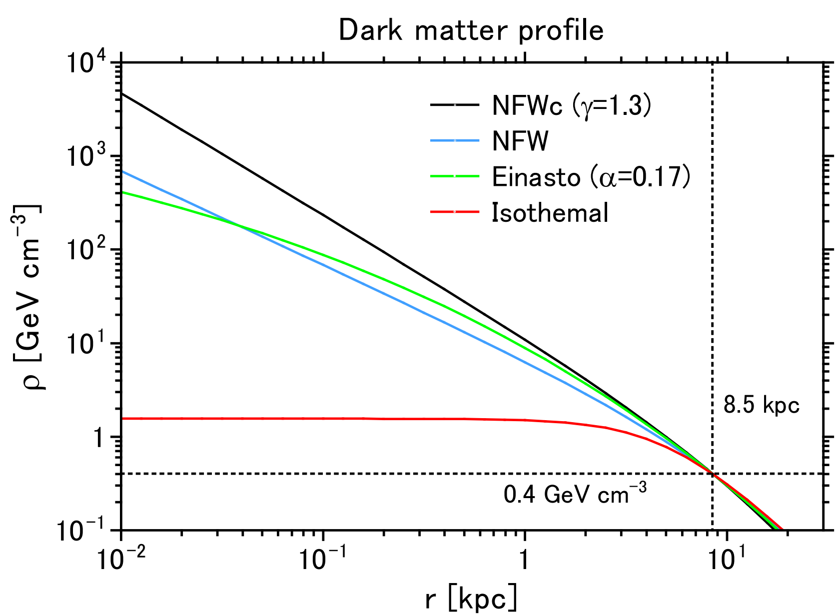

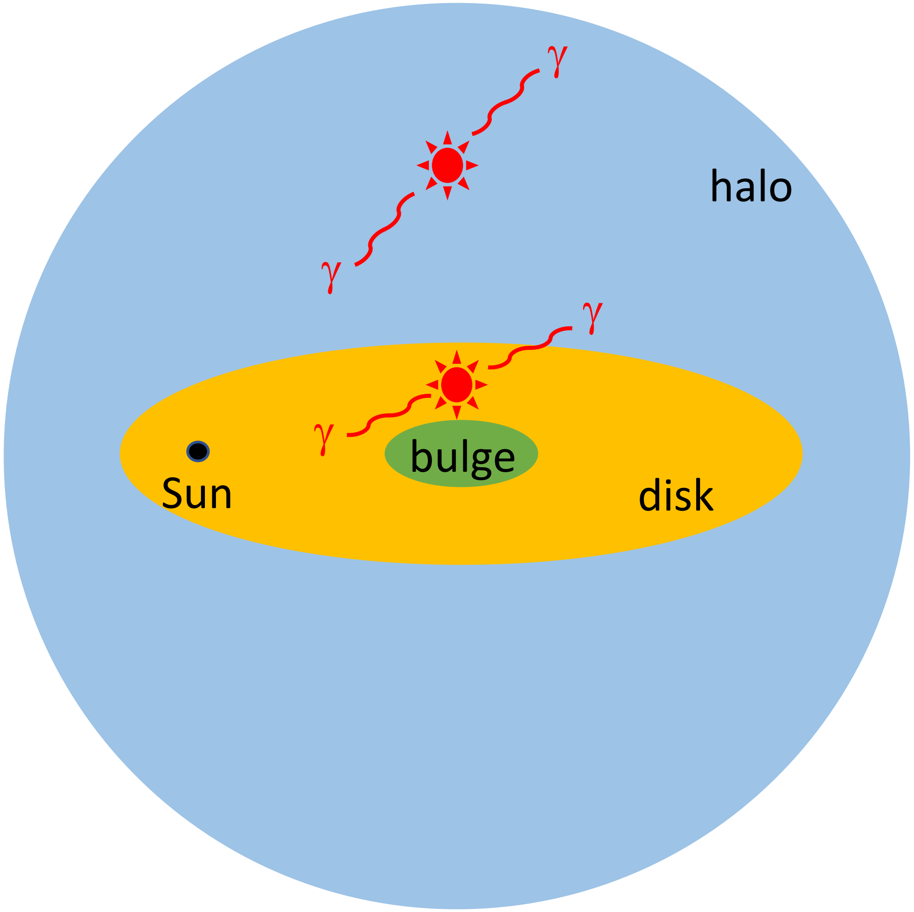

Profile is highly model dependent…
→ 4 models are assumed here.

Ref. Ackermann+, PR D91, 122002 (2015)

Regions of interest

(ROI)

Ref. Ackermann+, PR D91, 122002 (2015)

R (angular distance from GC)

<3° (NFWc profile) <41° (NFW profile)

<16° (Einasto profile) <90° (isothermal)

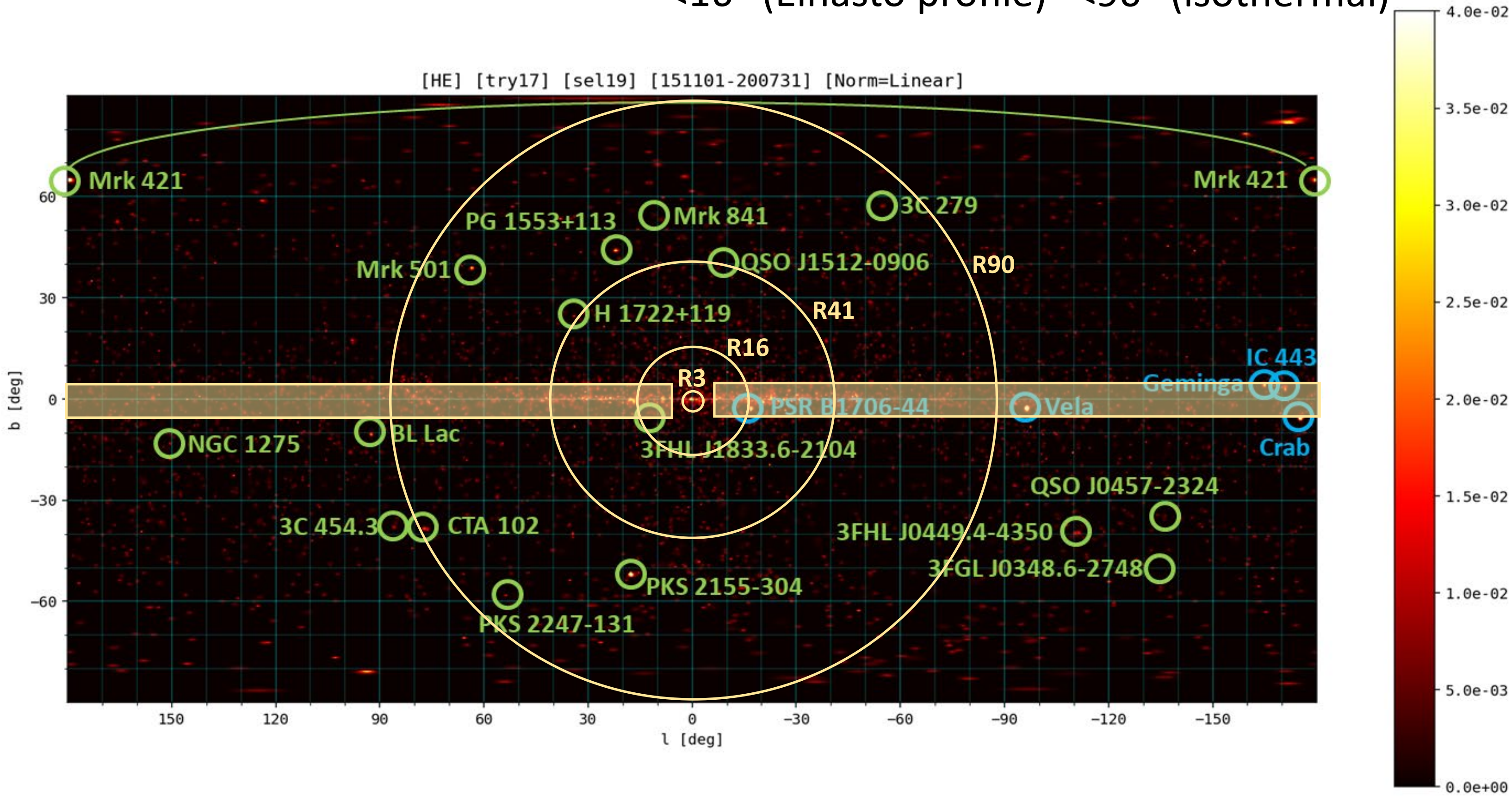

- Radius of ROI are optimized for each Galactic halo density profile model
- The disk regions ($|l|>6°$ and $|b|<5°$) and point sources are removed from analysis.

Dark matter density profile

Ackermann+, PR D91, 122002 (2015)

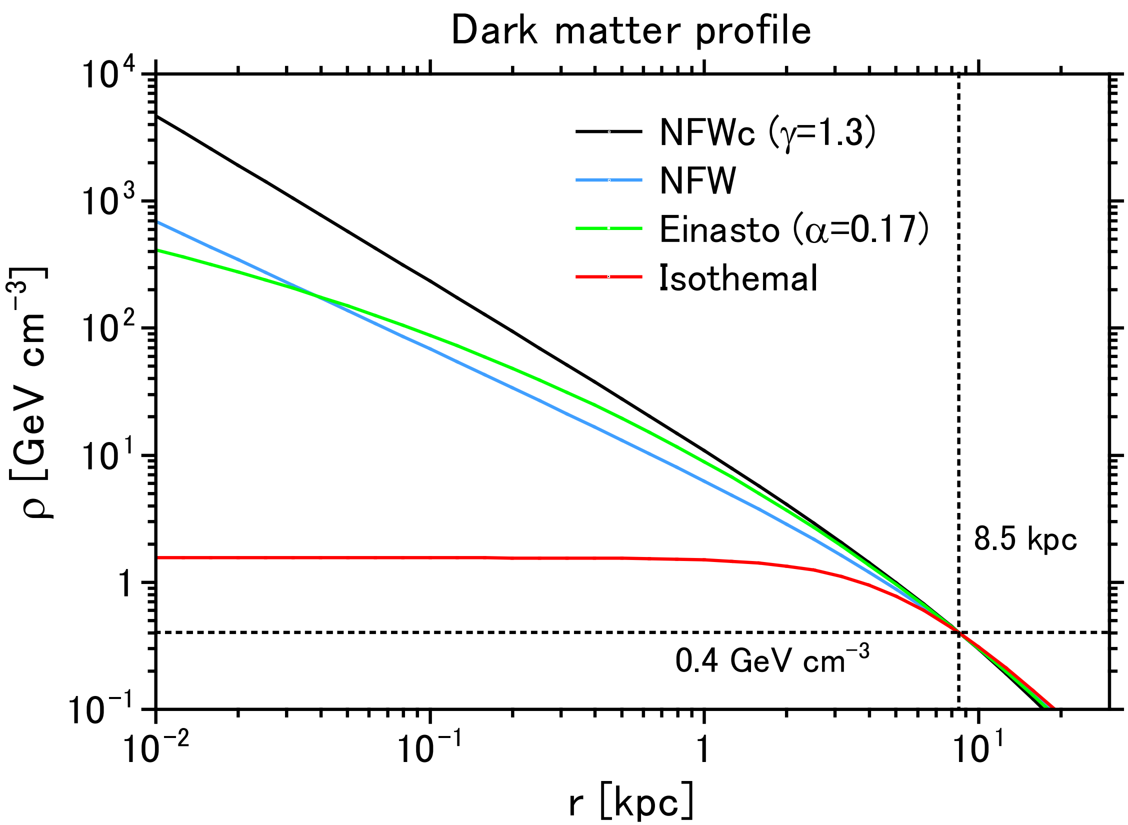

- Normalized to be 0.4 GeV cm^{-3} at 8.5 kpc from the Galactic center.
- Different densities are predicted around the Galactic center.

Line-of-sight profile

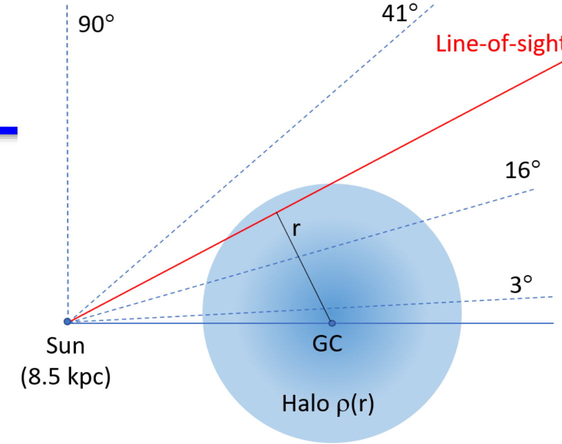

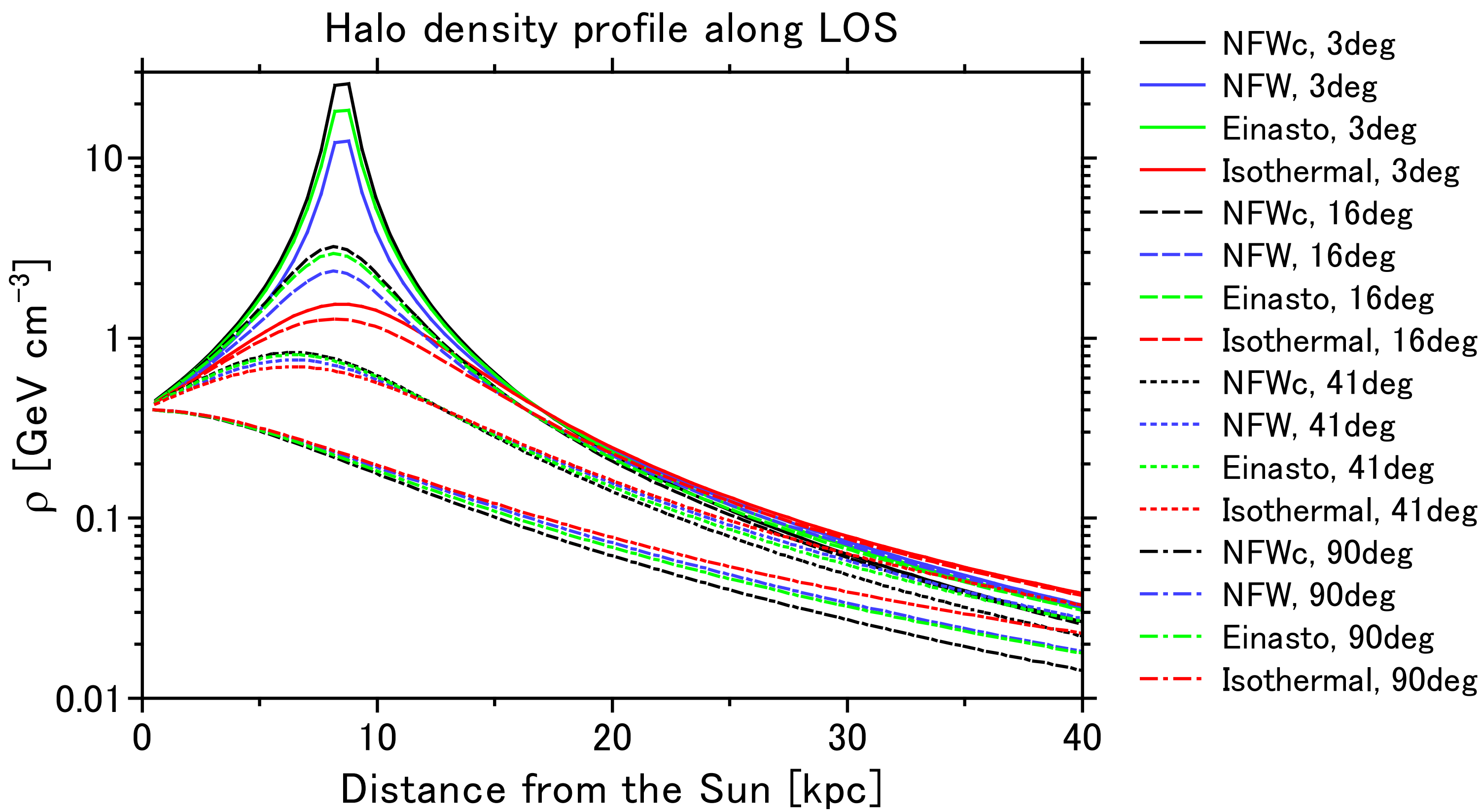

- We expect larger signals toward the Galactic center for cuspy profiles.

Calculation of upper limits

- Monoenergetic lines are assumed.
- Adding the assumed line signals (broadened by a Gaussian distribution with CALET energy resolution) to the observed spectra which raise the reduced χ^2 for the power-law fit by 3.94 (corresponding to 95% C.L.).

R16: E_{DM} = 39.8 GeV case

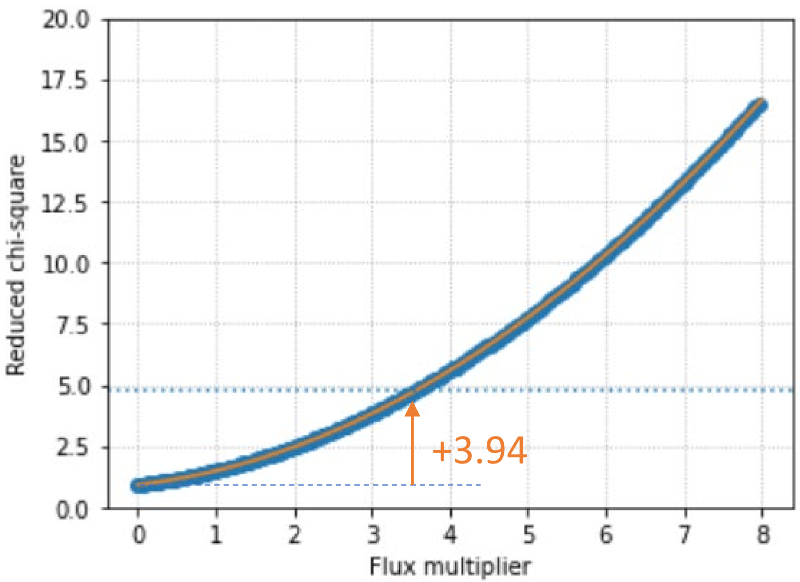

Assumed flux (unit: Power-law-fit)

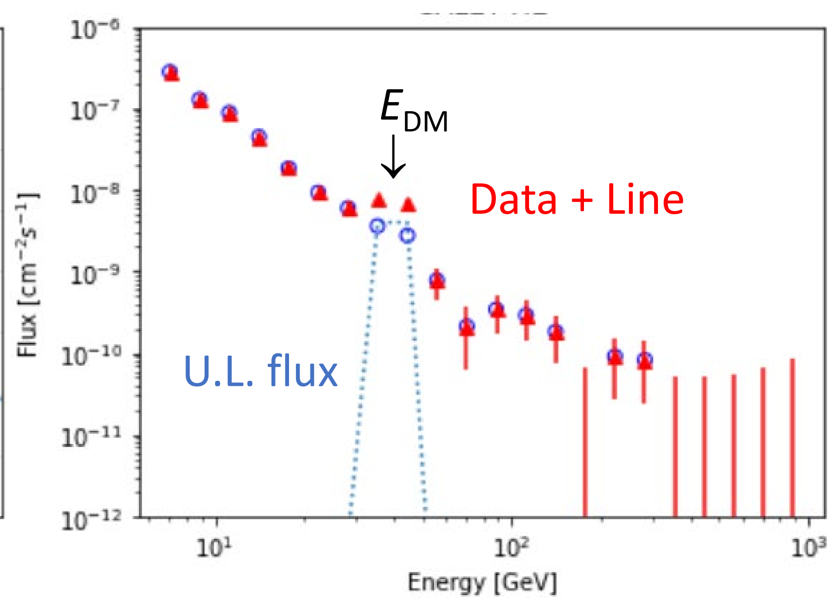

Upper limits as a function of energy

Mori et al., PoS(ICRC2021)619

Preliminary

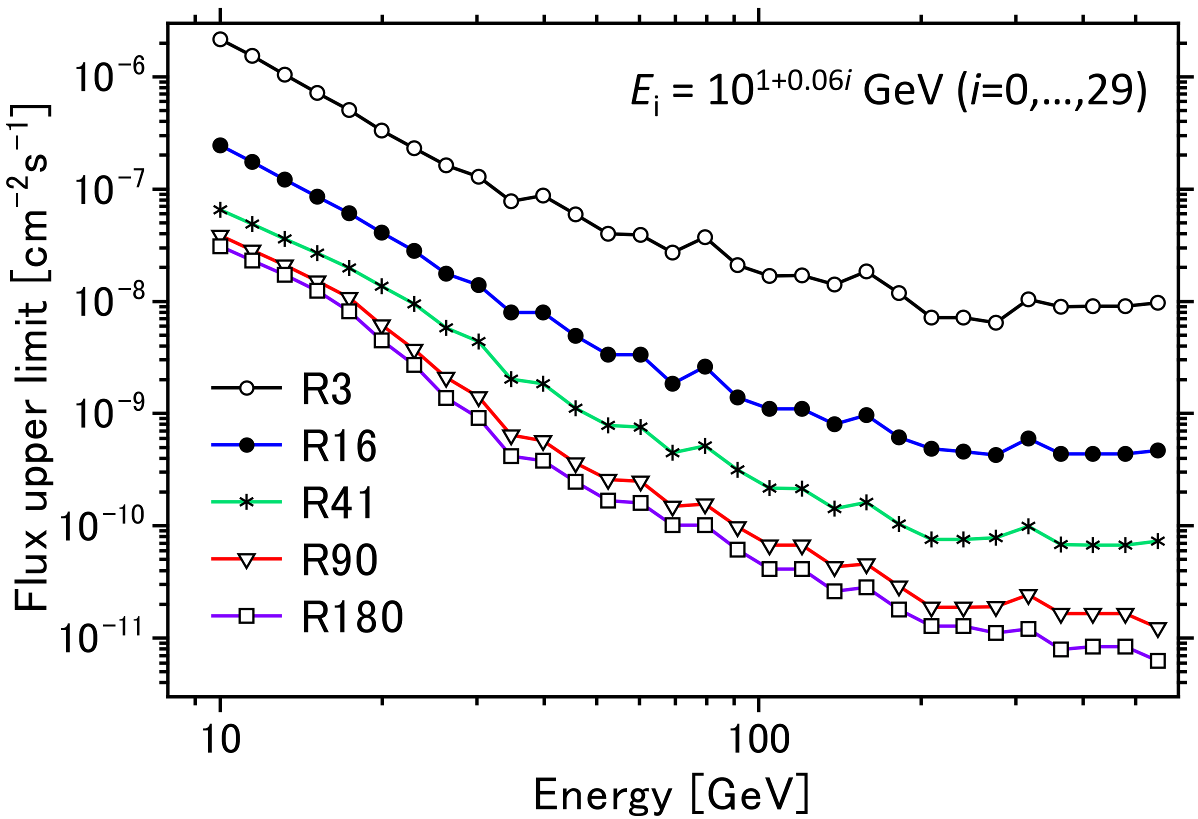

- Upper limits are mostly determined by event statistics.
- Systematic errors are not taken into account (under study).

Gamma-ray line signal from dark matter

- **Annihilation**

$$\left(\frac{\mathrm{d}\Phi}{\mathrm{d}E}\right)_{\mathrm{ann}} = \frac{\langle\sigma v\rangle}{8\pi m_{\mathrm{DM}}^2}\left(\frac{\mathrm{d}N}{\mathrm{d}E}\right)_{\mathrm{ann}}\left[\int_{\mathrm{ROI}}\mathrm{d}\Omega\int_{\mathrm{l.o.s.}}\mathrm{d}s\,\rho(r)^2\right]$$

<σv>: velocity-averaged cross section

$\mathrm{d}N/\mathrm{d}E = 2\delta(E_\gamma - E)$, $E_\gamma = m_{\mathrm{DM}}$

- **Decay**

$$\left(\frac{\mathrm{d}\Phi}{\mathrm{d}E}\right)_{\mathrm{dec}} = \frac{1}{4\pi\tau_{\mathrm{DM}} m_{\mathrm{DM}}}\left(\frac{\mathrm{d}N}{\mathrm{d}E}\right)_{\mathrm{dec}}\left[\int_{\mathrm{ROI}}\mathrm{d}\Omega\int_{\mathrm{l.o.s.}}\mathrm{d}s\,\rho(r)\right]$$

τ_{DM}: lifetime

$\mathrm{d}N/\mathrm{d}E = \delta(E_\gamma - E)$, $E_\gamma = m_{\mathrm{DM}}/2$

J-factors: $\left[\int_{\mathrm{ROI}}\mathrm{d}\Omega\int_{\mathrm{l.o.s.}}\mathrm{d}s\,\rho(r)^2\right]$, $\left[\int_{\mathrm{ROI}}\mathrm{d}\Omega\int_{\mathrm{l.o.s.}}\mathrm{d}s\,\rho(r)\right]$ halo-model dependent!

Integral of (halo density)^2 $\rho(\underline{r})^2$ [halo density $\rho(\underline{r})$] along line-of-sight (l.o.s.) over Region-of-Interest (ROI)

Upper limits on <σv>

Fermi-LAT: Ackermann+, PR D91, 122002 (2015)
H.E.S.S.: Abdallah+, PRL 120, 201101 (2018)
Thin line: thermal relic ($3\times10^{-26}cm^3s^{-1}$)

Mori et al., PoS(ICRC2021)619

Preliminary: statistical error only

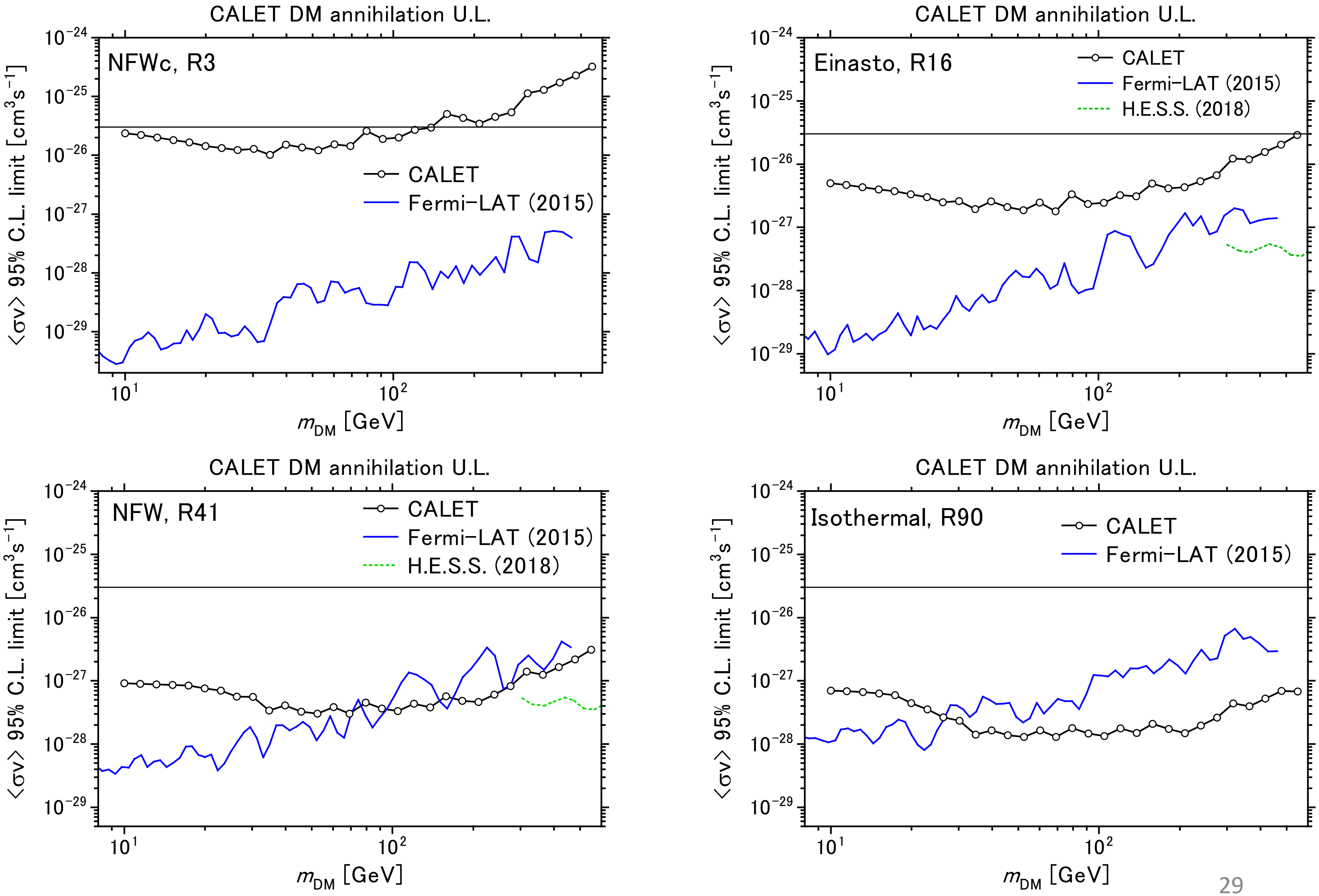

Upper limits on lifetime

Fermi-LAT: Ackermann+, PR D91, 122002 (2015)

Mori et al., PoS(ICRC2021)619

Preliminary: statistical error only

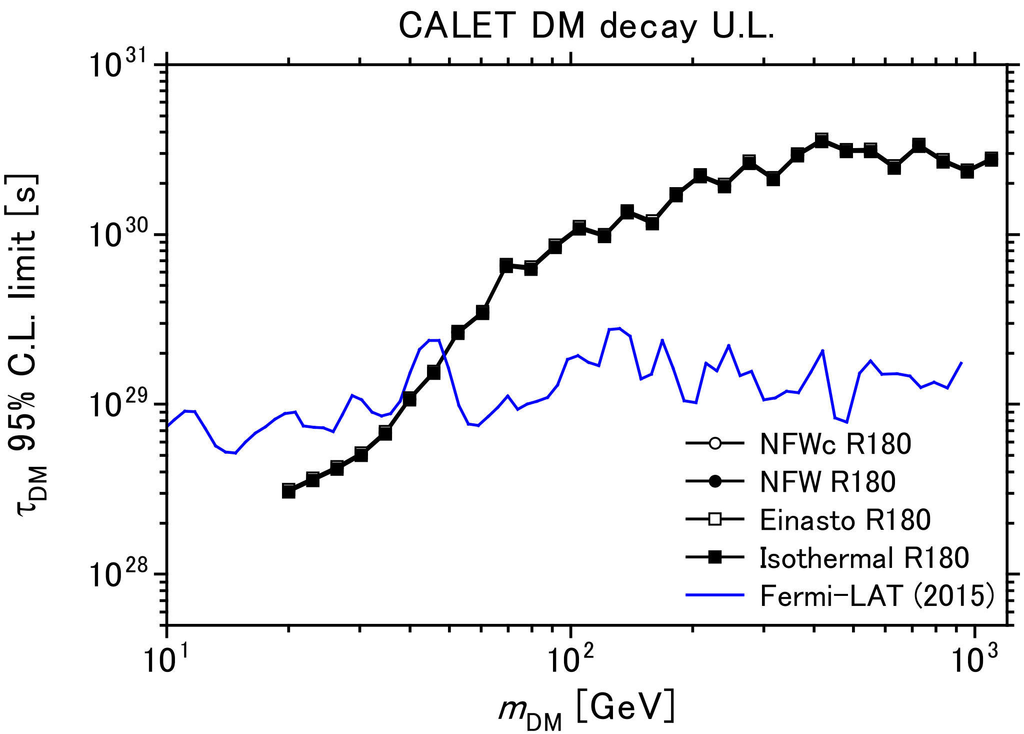

For R180, limits are almost independent of the profile models.

- Good energy resolution of CALET enables sensitive search at high energies, but limited by the statistics of observed gamma rays.
- Thus for larger ROI, we may set better upper limits.

Summary

- The CALET detector on ISS is monitoring the gamma-ray sky above 1 GeV with observations spanning more than six years since 2015.
- Diffuse gamma-ray fluxes and bright gamma-ray source spectra are consistent with Fermi-LAT observations.
- Gamma-ray events above 10 GeV have been analyzed to search for possible line signals utilizing good energy resolution of CALET.
    - We found no hint of line signals and gave upper limits on parameters of the DM annihilation and decay models for m_{DM} = 10 ~ 500 GeV.
    - We are now studying possible systematic errors in our limits.